Single-Molecule Conductance

DOI: 10.1002/anie.201100431

Electron Transport through Single Molecules Comprising Aromatic Stacks Enclosed in Self-Assembled Cages[**]

Manabu Kiguchi, Takuya Takahashi, Yuta Takahashi, Yoshihiro Yamauchi, Takashi Murase, Makoto Fujita,* Tomofumi Tada, and Satoshi Watanabe*

Understanding how electrons are transported through single molecules is an important challenge in molecular electronics.[1] Electron transfer in noncovalently bound, π-stacked systems has been of particular interest and plays a vital role in biological systems,[2] organic electronics,[3] polymer and materials science,[4] typically on the macroscopic level and in bulk.[5] However, electron transport through the initial building blocks of π-stacked systems has never been directly examined (although many experimental artifacts have been attributed to these small interactions) because creating molecular junctions of stacked π molecules between nanogap electrodes is nontrivial and sequential growing the π stack in a controlled manner typically requires extensive synthesis.[6]

Using conductance, inelastic electron-tunneling spectroscopy, and shot noise measurements, the Kiguchi group recently succeeded in directly measuring the single-molecule conductance of molecular junctions where a single π-molecule (benzene) was trapped and bound to platinum-metal electrodes without a conventional anchoring group (e.g. -SH group).[7] Meanwhile, the Fujita group has applied columnar coordination cages to efficiently and precisely assemble stacked π systems.[8] Herein, we combined these two techniques to obtain conductance measurements for π-stacked aromatics where the π stack was sequentially increased from four to six stacked aromatic molecules. We show that the conductance decreases with the increasing number of π systems but the decrease in conductance per electron transport distance is smaller than that of the conventional covalent, π-conjugated molecular junction.

Inclusion complexes $\mathbf{1}\cdot(\mathbf{4})_2$, $\mathbf{2}\cdot(\mathbf{4})_3$, and $\mathbf{3}\cdot(\mathbf{4})_4$, where the cavity height of the coordination cages **1**–**3** predetermines the number of π-stacked aromatic molecules **4**, were employed for the molecular junction conductance measurements (Figure 1 a). The inclusion complexes were prepared by simply mixing guest **4** with $[(\mathrm{en})\mathrm{Pd}(\mathrm{ONO}_2)_2]$ (**5**, en = ethylenedia-

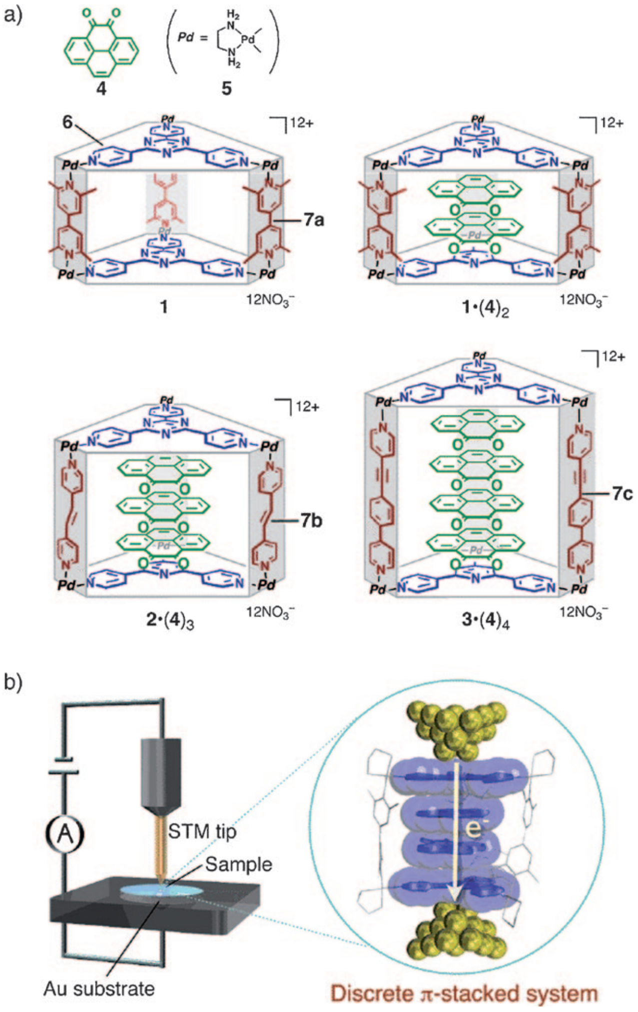

Figure 1. a) Structures of coordination cage **1** and π-stacked systems $\mathbf{1}\cdot(\mathbf{4})_2$, $\mathbf{2}\cdot(\mathbf{4})_3$, and $\mathbf{3}\cdot(\mathbf{4})_4$. b) The experimental setup for the conductance measurement.

---

[*] Dr. M. Kiguchi, T. Takahashi, Y. Takahashi
Department of Chemistry, Graduate School of Science and Engineering, Tokyo Institute of Technology
2-12-1 W4-10 Ookayama, Meguro-ku, Tokyo 152-8551 (Japan)
Fax: (+81) 3-5734-2242
E-mail: kiguti.m.aa@m.titech.ac.jp
Dr. Y. Yamauchi, Dr. T. Murase, Prof. Dr. M. Fujita
Department of Applied Chemistry, School of Engineering
The University of Tokyo
7-3-1 Hongo, Bunyo-ku, Tokyo 113-8656 (Japan)
Fax: (+81) 3-5841-7257
E-mail: mfujita@appchem.t.u-tokyo.ac.jp
Dr. T. Tada, Prof. Dr. S. Watanabe
Department of Materials Engineering, School of Engineering
The University of Tokyo
7-3-1 Hongo, Bunyo-ku, Tokyo 113-8656 (Japan)
T. Takahashi
Division of Chemistry, Graduate School of Science, Hokkaido University
N10W8 Kita, Sapporo, Hokkaido 060-0810 (Japan)

[**] We acknowledge support from the Ministry of Education, Science and Culture of Japan for Grant-on-Aid for Scientific Research on Priority Areas (Grant No. 17069001 and 20027003).

Supporting information for this article is available on the WWW under http://dx.doi.org/10.1002/anie.201100431.

mine), panel ligand **6**, and pillar ligand **7a–c** in water (typically, at 100 °C for 2 h).[8]

Using the direct binding nanogap technique, we measured the conductance of molecular junctions bridged by single molecules of inclusion complex **1**·(**4**)$_2$ trapped in the nanogap formed when gold leads are separated in the presence of the sample molecules. The complexes were trapped in the gold nanogap when a scanning tunneling microscope (STM) gold tip repeatedly moved into and out of contact with a gold substrate covered by a solution of the sample molecule (Figure 1 b).[9] The conductance traces obtained from gold contacts in a solution of **1**·(**4**)$_2$ are shown in Figure 2.

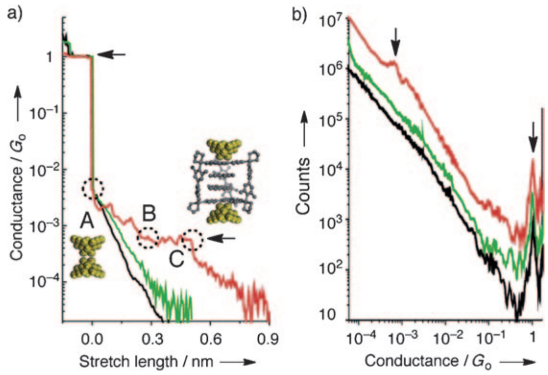

Figure 2. a) Typical conductance curves for inclusion complex **1**·(**4**)$_2$ (red), empty cage **1** (green), and aqueous blank (black). Position (A): breaking point of the Au junction, (B) formation of a molecular junction, (C) breaking of a molecular junction. b) The corresponding conductance histograms on a log–log scale. The histograms for **1** and **1**·(**4**)$_2$ are scaled by 2 and 8, respectively. The black arrows indicate peaks in the trace.

Immediately preceding separation of the gold electrodes, the conductance was 1 G_0 ($G_0 = 2e^2/h$, where e is the charge of an electron, and h is Plank's constant) and corresponds to an intact gold junction (point (A) in Figure 2 a).[10]

After breaking the gold junction, a new sequence of steps appeared in the lower conductance region owing to the formation of new molecular junctions. As the nanogap increases in size, at point (B) in Figure 2 a, a molecular junction is formed when a single π-stack molecule **1**·(**4**)$_2$ bridges the gap (see analysis of the conductance traces in the Supporting Information). The gap continues to increase until finally, the gap reaches point (C) where contact is lost. The corresponding conductance histogram (Figure 2 b) constructed from 1000 conductance traces showed a peak around $6\times10^{-4}\,G_0$ in addition to the clear 1 G_0 peak[11] (see Figures S1 and S2 in the Supporting Information). When a solution of empty cage **1** was measured, no plateaus or peaks were observed in the conductance traces or histograms between 0.03–$5\times10^{-5}\,G_0$ and the measured conductance behavior were quite similar to the blank aqueous solution. Thus, inclusion complex **1**·(**4**)$_2$ is conductive whereas empty cage **1** is indistinguishable from water and the observed conductance in **1**·(**4**)$_2$ is ascribed to electron transport through four π-stacked molecules (two molecules of guest **4** and two molecules of panel ligand **6**).

The conductance curves of π-stacked systems **2**·(**4**)$_3$ and **3**·(**4**)$_4$, consisting five and six stacked aromatics, were measured and compared (Figure 3 a–f). In all cases, plateaus were present in the conductance traces (indicated by arrows in Figure 3 a–c) at integer multiples: $6\times10^{-4}\,G_0$, $4\times10^{-4}\,G_0$, and $3\times10^{-4}\,G_0$ for **1**·(**4**)$_2$, **2**·(**4**)$_3$, and **3**·(**4**)$_4$, respectively. The conductance histograms constructed from 1000 conductance traces also showed peaks at the corresponding conductance values (Figure 3 d–f; see Ref. [11] and Supporting Information Figures S1 and S2). No plateaus or peaks were observed below $2\times10^{-4}\,G_0$ in the conductance traces or histograms. From repeated measurements, the conductance values of the

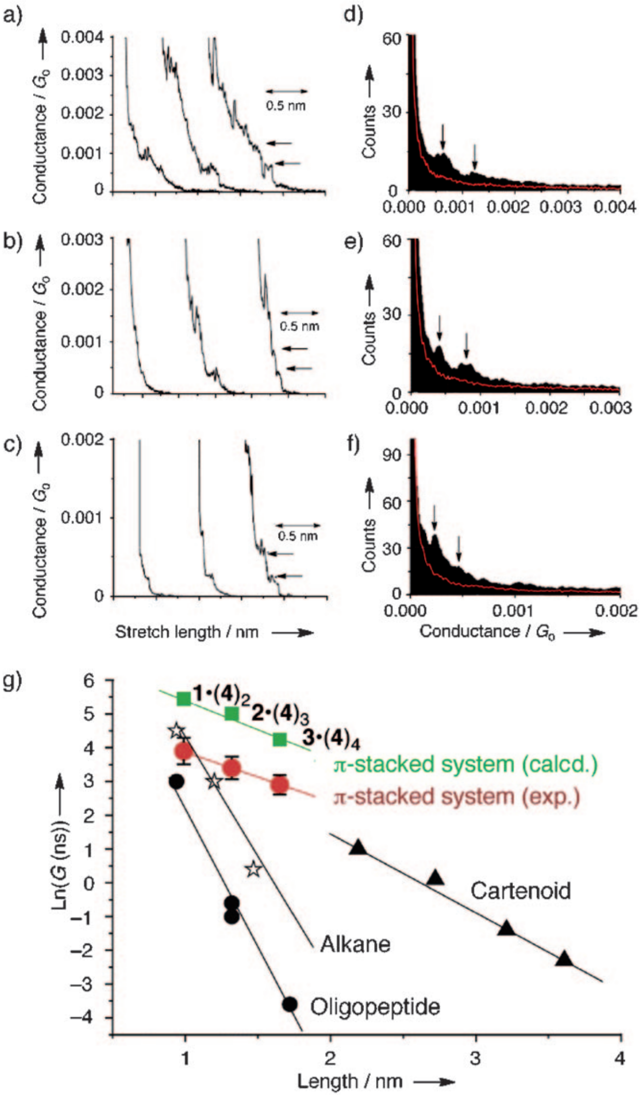

Figure 3. Conductance curves (a)–(c) and histograms (d)–(f) of Au electrodes in the π-stacked systems: a),d) **1**·(**4**)$_2$, b),e) **2**·(**4**)$_3$, and c),f) **3**·(**4**)$_4$. The red trace indicates the values obtained for the blank aqueous solution used as standard. g) The distance dependence of observed (exp) and calculated (calcd) conductance G for π-stacked systems **1**·(**4**)$_2$, **2**·(**4**)$_3$, and **3**·(**4**)$_4$. Typical single-molecule measurements for saturated (alkane chains and peptides) and conjugated (cartenoids) organic molecules are also shown.[1b]

molecular junctions of $\mathbf{1}\cdot(\mathbf{4})_2$, $\mathbf{2}\cdot(\mathbf{4})_3$, and $\mathbf{3}\cdot(\mathbf{4})_4$ were determined to be $6\pm3\times10^{-4}$, $4\pm2\times10^{-4}$, and $2.5\pm0.6\times10^{-4}\,G_0$, respectively.[12]

In general, the conductance (G) of a short molecular junction scales exponentially with length according to Equation (1)[1b,13]

$$G = A_N \exp(-\beta L) \qquad (1)$$

where A_N is a constant, L is molecular length, and β is the exponential pre-factor that depends on the electronic structure of the molecular junction. Since the β value roughly decreases with the decrease in HOMO–LUMO gap,[13d] conductive molecules have small β values whereas insulating molecules have large ones. The β value for the single-molecule π-stacked systems was determined to be 0.1 Å^{-1} from the slope of L versus ln$G$ plots (Figure 3g), smaller than that of insulating alkane chains (β = 0.7–0.9 Å^{-1}), and comparable to that of conductive π-conjugated organic molecules (β = 0.05–0.2 Å^{-1}).[1b]

Statistical analysis of the conductance traces indicated that the top and bottom panels **6** in the cages $\mathbf{1}\cdot(\mathbf{4})_2$, $\mathbf{2}\cdot(\mathbf{4})_3$, and $\mathbf{3}\cdot(\mathbf{4})_4$ (see Figure 1) bridge between the Au electrodes in the single-molecular junction. As shown in Figure 4a, the breaking distance (L_b) increased with increasing height of the π stack. The breaking distance is the distance between breaking point of the Au junction and that of the single-molecule junction. The L_b values roughly parallel the height of the cages and the incremental increase of L_b with increasing π-stacked length indicates the bridging of the electrodes along the long axis of the cages rather than the short axes. The length of the last plateau (L_m) indicates that the stability of the single-molecule π-stacked systems is similar to the Au–S linked molecular junctions formed by a single 1,4-benzenedithiol (Figure 4b).[9a] For a detailed explanation, see Supporting Information.

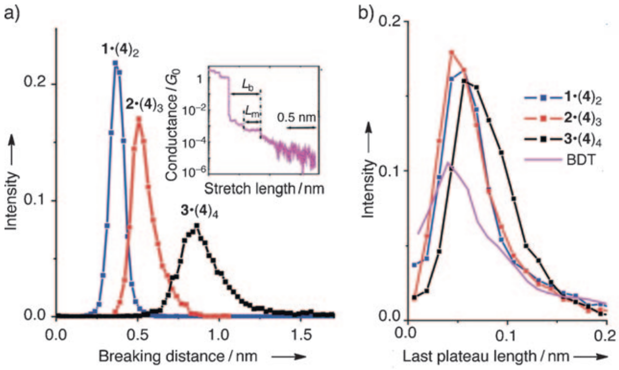

Figure 4. a) The distribution of breaking distances (L_b): inclusion complex $\mathbf{1}\cdot(\mathbf{4})_2$ (blue), $\mathbf{2}\cdot(\mathbf{4})_3$ (red), $\mathbf{3}\cdot(\mathbf{4})_4$ (black). Inset: the conductance curve of inclusion complex $\mathbf{1}\cdot(\mathbf{4})_2$, showing the data-point selection. b) The distribution of lengths of the last plateau (L_m) inclusion complex $\mathbf{1}\cdot(\mathbf{4})_2$ (blue), $\mathbf{2}\cdot(\mathbf{4})_3$ (red), $\mathbf{3}\cdot(\mathbf{4})_4$ (black), and 1,4-benzenedithiol (BDT purple).

Theoretical calculations based on the non-equilibrium Green's function method coupled with density functional theory, NEGF-DFT[14] supported our experimental findings. To reduce the calculation time, organic pillars **7** and $[(\mathrm{en})\mathrm{Pd}]^{2+}$ units were removed and aromatic stacks $(\mathbf{6})\cdot(\mathbf{4})_n\cdot(\mathbf{6})$ (n = 2–4) were used as simple models for $\mathbf{1}\cdot(\mathbf{4})_2$, $\mathbf{2}\cdot(\mathbf{4})_3$, and $\mathbf{3}\cdot(\mathbf{4})_4$, respectively. The conductance of stacks $(\mathbf{6})\cdot(\mathbf{4})_n\cdot(\mathbf{6})$ (n = 2–4) sandwiched between Au(111) electrodes was calculated from transmission profile in Figure 5a and the conductance values were plotted (Figure 3g). From the slope of the calculated conductance values, the β value for the single-molecule $(\mathbf{6})\cdot(\mathbf{4})_n\cdot(\mathbf{6})$ molecular junctions was estimated to be 0.13 Å^{-1}. This value is nearly identical to the obtained experimental β value and reinforces that, for inclusion complexes $\mathbf{1}\cdot(\mathbf{4})_2$, $\mathbf{2}\cdot(\mathbf{4})_3$, and $\mathbf{3}\cdot(\mathbf{4})_4$, electron transfer does primarily occur through the π-stacked systems.

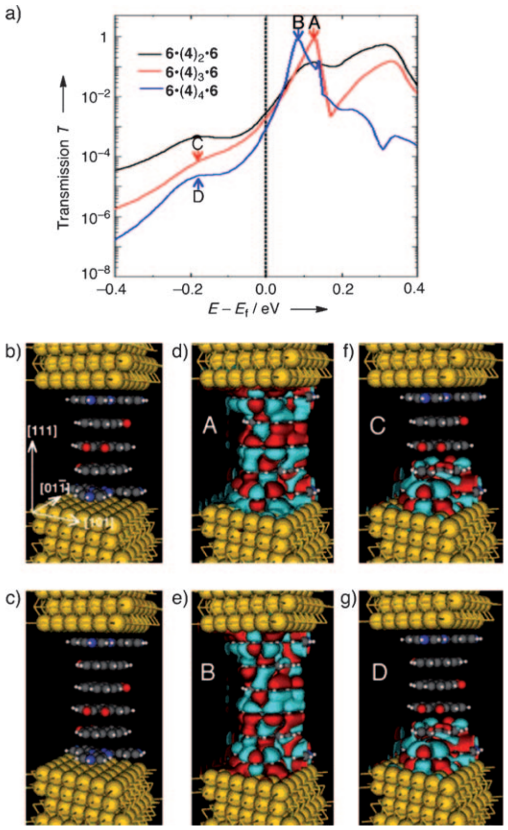

Figure 5. a) Calculated transmission curves for model π stacks $(\mathbf{6})\cdot(\mathbf{4})_2\cdot(\mathbf{6})$ (black), $(\mathbf{6})\cdot(\mathbf{4})_3\cdot(\mathbf{6})$ (red), and $(\mathbf{6})\cdot(\mathbf{4})_4\cdot(\mathbf{6})$ (blue). The simplified π-stacked models for b) $(\mathbf{6})\cdot(\mathbf{4})_3\cdot(\mathbf{6})$ and c) $(\mathbf{6})\cdot(\mathbf{4})_4\cdot(\mathbf{6})$; Au yellow, N blue, C gray, H white, O red. The unit cell size along the $[01\bar{1}]$ and $[\bar{1}01]$ directions is 17.28 (=2.88×6) Å, where 2.88 Å is the Au–Au bond length in bulk Au. d),e) LUMO and f),g) HOMO projected onto the top-most layers of Au electrodes and the model π stacks: d),f) $(\mathbf{6})\cdot(\mathbf{4})_3\cdot(\mathbf{6})$ and e),g) $(\mathbf{6})\cdot(\mathbf{4})_4\cdot(\mathbf{6})$. The difference of colors of orbitals (cyan/red) indicates the difference of the orbital phases. A,B and C,D indicate LUMO and HOMO, respectively, see text for more details.

The calculations confirm the efficient conductance of the π-stacked complexes. First, all $(\mathbf{6})\cdot(\mathbf{4})_n\cdot(\mathbf{6})$ assemblies have small HOMO–LUMO gaps (indicated by peaks C, D (HOMO) and A, B (LUMO) at −0.2 and +0.1 eV, respectively, in Figure 5 a) which are important for efficient conduction. Second, the orbital overlap between the neighboring molecules in the stack (0.01 for LUMO–LUMO) suffices for orbital-delocalization and electron-transport pathways (Figure 5 d,e). Finally, the in-phase (bonding) relationship between the panel ligand **6** and the Au(111) electrode surface in the HOMOs (Figure 5 f,g) supports the strong Au–π interaction (see Supporting Information).

In summary, we succeeded in directly measuring electron transport through single-molecular assemblies of π-stacked aromatics. Unlike previous systems where random aromatic–aromatic interactions between covalently π-conjugated "wires" leads to complicated and unclear results, in this case we can sequentially control the number and relative position of π-stacked aromatic molecules. Thus, for the first time, we were able to precisely calibrate the electron-transport distance and demonstrate that single-molecule π stacks exhibit good conductance with only a moderate loss of conductance with increasing transport length. These experimental results further show that molecular junctions can form without anchoring thiol groups, thus potentially simplifying the synthesis of organic molecular wires and adding a new method for measuring the conductance of complex single-molecule molecular junctions. Furthermore, they provide an experimental and theoretical foundation, at the single-molecule level, for the design and synthesis of molecular wires and devices where π-stacked aromatics provide the pathways for electron transport. It is important to note that these results were obtained only through the combination of synthetic, analytic, and theoretical chemical expertise.

Received: January 18, 2011

Keywords: electron transfer · molecular electronics · nanogap electrode · π interactions · single-molecule studies

---

[1] a) A. Aviram, M. A. Ratner, *Chem. Phys. Lett.* **1974**, *29*, 277–283; b) N. J. Tao, *Nat. Nanotechnol.* **2006**, *1*, 173–181; c) H. Song, Y. Kim, Y. H. Jang, H. Jeong, M. A. Reed, T. Lee, *Nature* **2009**, *462*, 1039–1043; d) I. Díez-Pérez, J. Hihath, Y. Lee, L. Yu, L. Adamska, M. A. Kozhushner, I. I. Oleynik, N. Tao, *Nat. Chem.* **2009**, *1*, 635–641.

[2] J. C. Genereux, J. K. Barton, *Chem. Rev.* **2010**, *110*, 1642–1662.

[3] a) S. Bhosale, A. L. Sisson, P. Talukdar, A. Fürstenberg, N. Banerji, E. Vauthey, G. Bollot, J. Mareda, C. Röger, F. Würthner, N. Sakai, S. Matile, *Science* **2006**, *313*, 84–86; b) N. Sakai, R. Bhosale, D. Emery, J. Mareda, S. Matile, *J. Am. Chem. Soc.* **2010**, *132*, 6923–6925.

[4] a) J. Wu, W. Pisula, K. Müllen, *Chem. Rev.* **2007**, *107*, 718–747; b) X. Feng, V. Marcon, W. Pisula, M. R. Hansen, J. Kirkpatrick, F. Grozema, D. Andrienko, K. Kremer, K. Müllen, *Nat. Mater.* **2009**, *8*, 421–426.

[5] a) M. Bendikov, F. Wudl, D. F. Perepichka, *Chem. Rev.* **2004**, *104*, 4891–4945; b) W. A. Schoonveld, J. Wildeman, D. Fichou, P. A. Bobbert, B. J. van Wees, T. M. Klapwijk, *Nature* **2000**, *404*, 977–980.

[6] a) S. Wu, M. T. González, R. Huber, S. Grunder, M. Mayor, C. Schönenberger, M. Calame, *Nat. Nanotechnol.* **2008**, *3*, 569–574; b) S. T. Schneebeli, M. Kamenetska, Z. Cheng, R. Skouta, R. A. Friesner, L. Venkataraman, R. Breslow, *J. Am. Chem. Soc.* **2011**, *133*, 2136–2139.

[7] M. Kiguchi, O. Tal, S. Wohlthat, F. Pauly, M. Krieger, D. Djukic, J. C. Cuevas, J. M. van Ruitenbeek, *Phys. Rev. Lett.* **2008**, *101*, 046801.

[8] Y. Yamauchi, M. Yoshizawa, M. Akita, M. Fujita, *J. Am. Chem. Soc.* **2010**, *132*, 960–966.

[9] a) M. Kiguchi, S. Miura, K. Hara, M. Sawamura, K. Murakoshi, *Appl. Phys. Lett.* **2006**, *89*, 213104; b) A. Mishchenko, L. A. Zotti, D. Vonlanthen, M. Burkle, F. Pauly, J. C. Cuevas, M. Mayor, T. Wandlowski, *J. Am. Chem. Soc.* **2011**, *133*, 184–187.

[10] N. Agraït, A. L. Yeyati, J. M. van Ruitenbeek, *Phys. Rep.* **2003**, *377*, 81–279.

[11] The various conductance steps in traces and conductance peaks in histograms were found in the conductance region below 1 G_0. These steps and peaks correspond to the molecule junctions with different numbers of π-stacked molecules and/or different atomic configurations. In the present study, we attribute the last conductance step and first peaks to the single π-stacked molecule bridging Au electrodes with a certain fixed atomic configuration. The conductance histograms were constructed from conductance traces containing well-defined steps (see Supporting Information).

[12] In the present study, one data set of the conductance measurements consists of 1000 conductance traces. For each system, we collected three data sets for five independent samples, that is, 15000 conductance traces in total. The conductance of the single-molecule junction was determined by averaging all 15 data sets (see Supporting Information).

[13] a) X. Li, J. He, J. Hihath, B. Xu, S. M. Lindsay, N. Tao, *J. Am. Chem. Soc.* **2006**, *128*, 2135–2141; b) X. Xiao, B. Xu, N. Tao, *J. Am. Chem. Soc.* **2004**, *126*, 5370–5371; c) G. Sedghi, K. Sawada, L. J. Esdaile, M. Hoffmann, H. L. Anderson, D. Bethell, W. Haiss, S. J. Higgins, R. J. Nichols, *J. Am. Chem. Soc.* **2008**, *130*, 8582–8583; d) T. Tada, K. Yoshizawa, *J. Phys. Chem. B* **2004**, *108*, 7565–7572.

[14] a) M. Brandbyge, J. Mozos, P. Ordejón, J. Taylor, K. Stokbro, *Phys. Rev. B* **2002**, *65*, 165401; b) ATK Manual "ATK version 2008.10", QuantumWise A/S (www.quantumwise.com).